Phonon and Plasmon Interactions in Metal-Semiconductor Tunneling Junctions

M. Mikkor and W. C. Vassell

Scientific Research Staff, Ford Motor Company, Dearborn, Michigan 48121

(Received 27 March 1970)

Reproducible metal–semiconductor tunnel junctions are made on degenerate semiconductor single crystals whose surfaces have been cleaned by etching and then heating the samples in vacuum. This technique has been successfully used on GaAs, GaSb, and CdS. Detailed tunneling spectra are presented on the above-mentioned semiconductors and also on degenerate SnO_2. In addition, some of the metal–semiconductor junctions have been intentionally doped with molecular impurities. No identifiable vibrational spectra of the molecules are observed.

INTRODUCTION

Several studies of tunneling through the metal-semiconductor junctions of GaAs and CdS have been recently reported.[1-4] Considerable amounts of structure is observed in the voltage range 0–100 mV. This structure can be associated with the superconducting density of states phonons of the metal, as well as with the normal-metal phonons. Structure also occurs at the LO and TO phonon energies of the semiconductor. This has been attributed to self-energy effects,[5] and to hole-TO-phonon interactions.[2] At higher energies there is a broad structure which varies with the carrier concentration and has been associated with the free electron plasma mode in the semiconductor.[6,7]

In the present paper we present a way of making reproducible evaporated metal-semiconductor junctions and present detailed data on undoped junctions made on degenerate n- and p-type GaAs, and n-type CdS, GaSb, and SnO_2. In addition to this we have deliberately doped these junctions with molecular impurities as has been done with metal-oxide–metal junctions[8] in an attempt to observe the vibrational modes of the impurities.

EXPERIMENTAL METHODS

A. Sample Preparation

Care in preparation of a semiconductor surface before the evaporation of metal contacts or electrodes is important if reproducible tunnel junctions are to be obtained.

If the crystals have a cleavage plane, then one of the best ways of making a metal junction on an uncontaminated surface of the crystal is to cleave the crystal in high vacuum (10^{-9}–10^{-10} Torr) in a stream of evaporating metal. This has been successfully done on CdS by Wolf and Losee.[3] Evaporation on vacuum-cleaved surfaces of GaAs has also been done by Steinrisser.[6] This technique is not suitable if junctions are to be made on faces other than the cleavage planes or if one needs

large flat surfaces. Therefore, it is useful if one can prepare suitable surfaces by some other techniques.

Most of our junctions are prepared on mechanically polished and chemically etched surfaces of the semiconductor. In this case one has to consider the surface damage done by polishing, possible chemical compounds that may be left on the surface by different etches and the contamination of the surface by adsorbed gas atoms.

GaAs. In this case the mechanically damaged layer due to grinding and polishing is roughly equal to the diameter of the final grinding particles.[9] The depth of damage varies with crystal orientation, and also depends on the particular III-V compound itself. The depth of damage being greatest for InSb and least for GaAs, i.e., InSb > InAs > GaSb > GaAs, for the same amount of cold-working.[10] This damaged layer can be removed by chemical etching. In n-type GaAs the defect states produced by mechanical grinding act as electron traps. This has been shown by Jones[9] in infrared reflection measurements. As the damaged layers of surface are removed the reflectivity minimum shifts toward shorter wavelength indicating increase in the number of free carriers at the surface. Thus, at least in principle, the amount of mechanical damage can control the carrier concentration on the surface and thus the semiconductor barrier thickness.

An example where a chemical polish may leave a residue on the crystal surface occurs when GaAs is etched with nitric acid. The nitric acid dissolves GaAs by forming a soluble gallium compound and As_2O_3. Arsenic trioxide is insoluble in nitric acid but soluble in water. Thus if water near the surface of the crystal becomes saturated, As_2O_3 crystals may form on the surface of GaAs.[11] Thus a careful washing of the crystal in water is necessary to remove As_2O_3. Arsenic trioxide also sublimes at 193 °C.

The adsorbed gases on the surface of the crystal

can be removed by heating the crystal in vacuum. This technique has been used in low-energy–electron-diffraction (LEED) studies of surfaces. LEED work on GaAs shows that samples which are polished, etched, and heated to 550 °C in vacuum give the same sharp diffraction pattern as vacuum-cleaved crystals. If the vacuum-cleaved crystals are exposed to the atmosphere, the diffraction pattern is deteriorated but can be restored by heating the crystal in vacuum. [12-14] This agrees with Thurmond's[15] statements that GaAs should evaporate congruently at temperatures below 660 ± 100 °C. The cleaning of surfaces of doped semiconductors by heating in vacuum raises the prospect of diffusion of the dopant out of the semiconductor. This problem should be carefully considered if the exact number of carriers present in the crystal is required for quantitative results. However, this may not be too important if the rate of congruent evaporation is much faster than the diffusion of impurities.

Since GaAs has a zinc-blende structure, the (111) faces present alternating layers of Ga and As atoms and the opposite planes have different surface atoms. Most of our junctions on GaAs are made on the (111) plane.

The following procedure is used in the sample preparations. The samples are mechanically polished using a 3-μ and then a 1-μ diamond paste on a polishing wheel. The polished samples are then cleaned ultrasonically in trichloroethylene and etched in CP-4 to remove the damaged surface layers. This is followed by a rinse in distilled water, a brief chemical polish in 1HF : 3HNO$_3$: 4H$_2$O solution, and another rinse in distilled water. The samples are then mounted in a stainless steel holder and placed in the vacuum system where they are heated to about 500–550 °C for 20 min in a vacuum of 10^{-6}–10^{-7} Torr. The samples are cooled to room temperature before evaporation of the metal electrodes.

Figure 1 illustrates the effect that a surface preparation can have on the current-voltage characteristics of a junction. The electrodes are 3-mm-diam lead dots evaporated on the same piece of n-type GaAs, having carrier concentration ~5 ×10^{18} per cm^3. The current-voltage characteristics are taken at liquid-helium temperature. The top curve shows the I - V plot of Pb-GaAs junction prepared on GaAs crystal that has been polished, etched, and heated in vacuum. The junction impedance is approximately $\frac{1}{10}$ Ω. The middle curve shows the characteristics of a junction that has been prepared exactly the same way as the previous one, except that after cooling the sample to room temperature it was exposed to atmosphere for about 20 min before evaporation of the lead
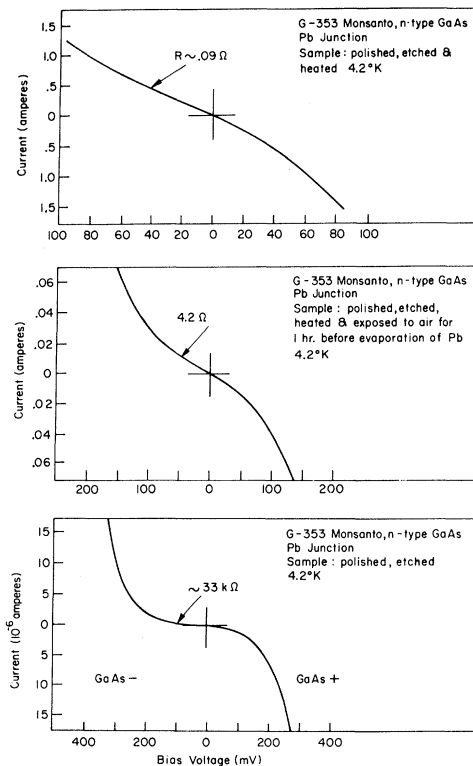

FIG. 1. Effect of surface preparation of GaAs on the current-voltage characteristics of the Pb-GaAs junctions at 4.2 °K. The carrier concentration of the n-type GaAs(Se) is 5.5×10^{18} cm^{-3}. The lowest junction impedances are obtained on samples heated in vacuum before evaporation of the metal electrodes.

electrode. Junctions made this way have impedances ranging from a few ohms up to about 100 Ω. The impedances are consistently much higher than for unexposed samples indicating that oxidation or gas adsorption takes place on the surface of the crystal. This layer of foreign atoms on the crystal surface acts as an additional tunneling barrier when the crystal is cooled down. The room-temperature impedances for exposed samples are seven or eight times smaller than at helium temperature and almost all of the resistance increase occurs between room temperature and 77 °K.

The bottom curve shows the I - V plot of a junction made on a polished and etched surface of GaAs which was not heated in vacuum. The sample impedance is about 30 kΩ near zero bias. The high impedance may be due to a thin layer of As$_2$O$_3$ that could have been left on the surface after an etch in nitric acid, although the sample was rinsed in distilled water after the etch. In contrast to the other two junctions, this junction shows no superconducting lead gap.

GaSb. The gallium antimonide crystals were

prepared the same way as the GaAs crystals. The crystals were polished, cleaned in trichloroethylene, etched in CP-4, and rinsed in distilled water before heating to 500 °C in the vacuum system. The crystals were then cooled to room temperature before evaporation of the metal electrodes, usually on the (111) faces of the crystal.

CdS . Cadmium sulfide, like all II-VI compounds, has a stable hexagonal wurtzite structure. In wurtzite structure the (0001) surfaces present alternating layers of group-II and group-VI atoms. These are usually called *A* and *B* faces. In CdS the *A* face would have Cd atoms on the surface, and the *B* face the S atoms. The faces can be distinguished from each other by etching. The cadmium face is smooth and shiny with well developed hexagonal pits while the sulfur face appears matte and irregular.[16] This is similar to the (111) surface of III-V compounds which also present alternating layers of different atoms.

LEED experiments by Campbell and Farnsworth[17] have shown that it is not possible to clean the surfaces of CdS crystals, previously exposed to air completely by heating alone. Half-orders of the diffraction pattern which are observed in vacuum-cleaved surfaces cannot be restored on air exposed surfaces even if samples are heated up to 500 °C in vacuum. Shappir and Many[18] report that at temperatures as high as 500 °C in high vacuum the chemiabsorbed oxygen is not desorbed and that prolonged illumination with intense ultraviolet light across the band gap is necessary to desorb all the oxygen. If crystals are heated to temperatures much higher than 500 °C, faceting of crystal surfaces occur. Schubert[19] reports, however, that some of the adsorbed oxygen is driven off at temperatures as low as 220 °C.

The barrier height of CdS is mainly dominated by the work function of the metal.[20] This is in contrast to GaAs where the barrier is almost independent of the work function of the metal and is surface-state dominated. Clean surfaces of CdS are essentially free of acceptorlike surface states and the bands are essentially flat.[21] Surfaces exposed to oxygen or air have barrier heights of about 0.5 V at atmospheric pressure. The oxygen attached to the surface acts as an acceptorlike surface state. Desorption of oxygen by uv light in vacuum will bring the barrier height down to as low as 0.06 V.[18] Our junctions on CdS were made by evaporating the metal electrodes directly on air-cleaved faces parallel to the *c* axis. Some junctions were also made on slices cut perpendicular to *c* axis. The latter were mechanically polished, cleaned ultrasonically in trichloroethylene, then etched in 2HCl: H_2O, and rinsed in distilled water. The samples are then heated to about 300 °C in vacuum for

approximately 20 min and cooled to room temperature before evaporation of the metal. No difference in the structure of d^2I/dV^2 spectra was observed between the air-cleaved and the chemically etched and heated surfaces.

SnO_2. Experiments on tin oxide were performed using Sb-doped single crystals. These crystals as grown have a 25–50-μ-thick insulating layer which was removed by grinding with 600 grit Al_2O_3.[22] The crystals were then ultrasonically cleaned before evaporation of electrodes on faces parallel to the *c* axis. In contrast to the other materials used it was not necessary to polish, etch, and heat in vacuum in order to obtain reproducible tunnel junctions.

B. Measurement Techniques

The detection of small changes in conductivity using second-derivative techniques is well known.[23] We are using a circuit similar to one used by Lambe and Jaklevic[8] to measure d^2I/dV^2 as a function of applied dc bias voltage. The schematic of the circuit is shown in Fig. 2. A small 50-kHz ac modulating voltage $V_0 \cos\omega t$ is applied across the junction as the bias voltage V is slowly varied. The second harmonic voltage at frequency 2ω or 100 kHz is detected by a synchronous detector. A transformer is used to match the impedances of the junctions to the optimum input impedance of the preamplifier. A 50-kHz notch filter is used to prevent the overloading of the preamplifier by the modulating signal. The ac and dc parts of the circuit are isolated from each other by chokes and capacitors. This can be done very effectively at high frequencies.

In many cases our junction impedances were of the order of a few ohms and varied considerably over the voltage range of interest. In order to keep the modulating voltage $V_0 \cos\omega t$ across the junction constant as the bias voltage is changed a
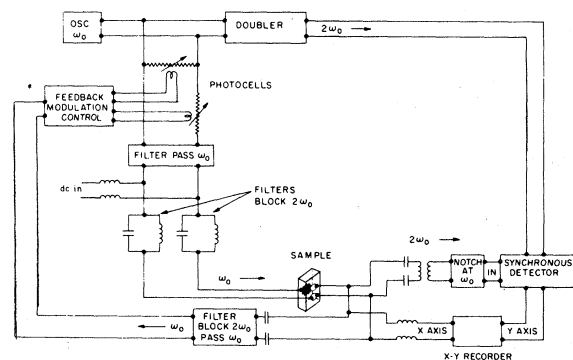

FIG. 2. Schematic of the circuit for taking the second derivative d^2I/dV^2.

simple feedback system was designed. It consists essentially of two photo cells connected in series and in parallel across the oscillator. The resistances of these cells are controlled by two light bulbs whose outputs are 180° out of phase with each other. The light intensity of the bulbs are in turn controlled by the amplitudes of ac modulation across the sample. The use of photoresistors as controlling elements of the modulation signal essentially eliminates the problems of electronic pickup and extraneous noise being introduced from feedback system into the ac drive circuit.

The second harmonic voltage generated by the junction is proportional to d^2I/dV^2 times the sample impedance $R_s = dV/dI$ at given bias voltage V. This can be seen by expanding the total voltage V_T across the junction in a Taylor series as a function of current,

$$V_T = f(I + I_{ac}) = f[I + (V_0/R_s)\cos\omega t],$$

where I is the direct current through the junction due to the dc bias voltage V and $I_{ac} = (V_0/R_s)\cos\omega t$ is the current due to the constant modulating voltage $V_0 \cos\omega t$. Thus,

$$V_T = V + \frac{V_0}{R_s}\cos\omega t \frac{dV}{dI} + \frac{1}{2!}\frac{V_0^2}{R_s^2}\cos^2\omega t \frac{d^2V}{dI^2} + \cdots$$

$$= \left(V + \frac{1}{4}\frac{V_0^2}{R_s^2}\frac{d^2V}{dI^2} + \cdots\right) + \frac{V dV}{R_s dI}\cos\omega t$$

$$+ \frac{1}{4}\frac{V_0^2}{R_s^2}\frac{d^2V}{dI^2}\cos 2\omega t + \cdots,$$

where the second harmonic voltage appearing across the junction is

$$V(2\omega) = \frac{1}{4}\frac{V_0^2}{R_s^2}\frac{d^2V}{dI^2}\cos(2\omega t)$$

because

$$R_s = \frac{dV}{dI}$$

and

$$\frac{dV}{dI} = 1\bigg/\frac{dI}{dV} \quad \frac{d^2V}{dI^2} = -R_s^3\frac{d^2I}{dV^2} \ .$$

Thus,

$$V(2\omega) = \tfrac{1}{4}V_0^2 R_s\frac{d^2I}{dV^2}\cos(2\omega t).$$

Usually R_s is very slowly varying compared to d^2I/dV^2 and in most cases can be taken as constant. It should be noted that all of our curves as shown are actually plots of $R_s d^2I/dV^2$ and not strictly speaking of just d^2I/dV^2. In most cases it makes no difference except in the case of p-type GaAs at

reverse bias where it introduces a noticeable correction to the background.

All the measurements are made at 4.2 to 1.2 °K. The samples are immersed directly into liquid-helium bath. A three-probe method of measurement is used.[24] This method eliminates the need to have an Ohmic contact for one of the current leads, and also most of the voltage drop across the bulk of the crystals is not measured. In the two-probe measurements one has to have an Ohmic contact for one of the current leads since the voltage measured is across all of the crystal. The arrangement of the electrodes is shown in Fig. 3. Two metal contacts are evaporated on one side of the crystal and a large low-impedance metal contact on the other side. The current is passed through the large contact (3) on the backside and through one of the junctions under study (1) on the other side of the crystal. The voltage is measured between the contact (1) and another metal contact (2) on the same side of the crystal. All the leads are put on the metal contacts with silver paint (Microdot SC-12), care being taken that the silver paint islands for the current and voltage leads on contact (1) do not overlap. This eliminates any voltage drop between the silver paint and the metal electrode from the measurement. The potential at contact (1) is the potential of the metal electrode and the potential at contact (2) is essentially the potential at distance λ from the surface of the semiconductor, where λ is the depth of depletion region. This is true as long as the junction impedance of the Schottky barrier is large compared to the bulk impedance of the crystal. If, however, the junction impedance becomes comparable to that of the bulk, then the measured voltage includes the voltage drop across the depletion layer and also part of the drop across the bulk of the sample. This can shift the observed structure in I-V plots to higher voltages. Thus the LO phonon structure would appear at voltages higher
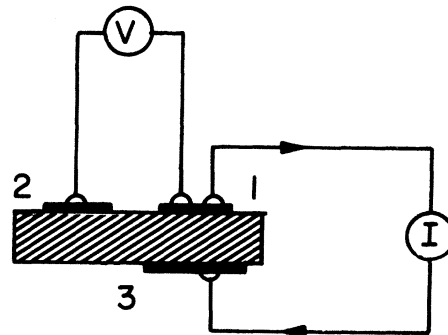

FIG. 3. Schematic showing the electrode arrangements on the sample.

than 37.5 mV. We have actually observed this in
very low-impedance contacts where the LO phonon
has appeared at voltages as high as 45–50 mV. In-
creasing the junction resistance by simply cutting
down the contact area will shift the phonon back
toward 37.5 mV. Thus even with the method used
here the junction impedance should be considerably
higher than the bulk impedance of a layer of the
same thickness as the depletion layer.

EXPERIMENTAL RESULTS

The d^2I/dV^2 spectra of tunnel junctions made on
GaAs, GaSb, CdS, and SnO$_2$ are presented. Table
I summarizes the materials on which we have been
able to observe a superconducting Pb gap. In some
cases the samples were highly degenerate and the
metal-semiconductor-junction impedances were
very low. In these cases we were only able to
cover a voltage range of ±10 mV. However in all
cases shown in the table we were able to observe
a definite Pb gap which could be quenched by a
magnetic field.

A. Clean Junctions

1. *n-Type* GaAs

Measurements were made both on selenium- and
tellurium-doped GaAs single crystals obtained from
Monsanto. The nominal room-temperature carrier
concentrations given by Monsanto are 5.9×10^{18}
per cm^3 for Te-doped samples and 5.5×10^{18} per
cm^3 for Se-doped samples. The electrodes were
usually deposited on the 111 faces of the crystals.
The tunneling spectra were independent of whether
the electrodes were put on the A (Ga) face, B (As)
face, or on faces perpendicular to the 111 plane.
Tunneling junctions were made using Pb, Al, Sn,
and Au, all showing the same basic spectra of
GaAs in addition to the characteristic spectra of
the metal.

Curve (a) of Fig. 4 shows a typical second-deriv-
ative spectra of a Pb junction taken at 1.2 °K. The
antisymmetrical structure between 0 and ±20 mV
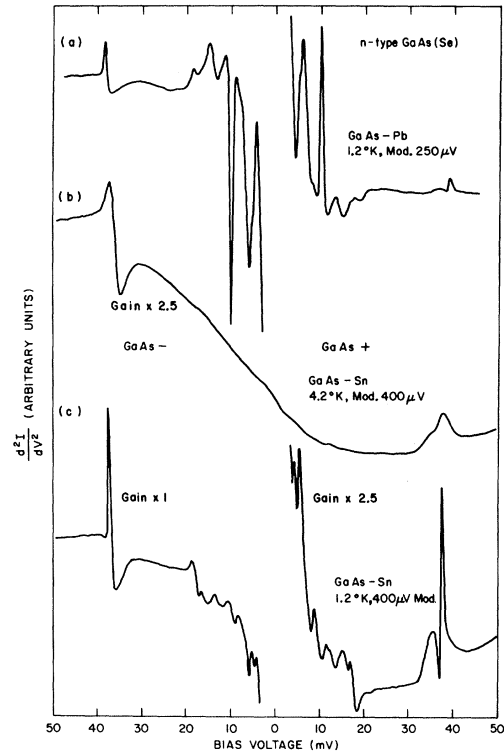is due to the density of states of the superconducting

TABLE I. List of semiconductors on which tunneling
was verified by observation of the superconducting lead
gap.

Material	Type	Pb Gap
GaAs	n, p	yes
GaSb	n	yes
InSb	p	yes
CdS	n	yes
SnO$_2$	n	yes
In$_2$O$_3$	n	yes
ZnO	n	yes

FIG. 4. Tunneling spectrum from Pb and Sn junctions
on n-type GaAs(Se). Curve (a) shows the spectra of
Pb-GaAs junction at 1.2 °K. Structure between 0 and
±20 mV is due to the density of states of superconducting
lead. The structure at ±38 mV is associated with the
LO phonon of GaAs. Curves (b) and (c) show the spectra
of Sn-GaAs junctions at 4.2 °K (Sn normal) and 1.2 °K
(Sn superconducting). The structure between ±20 mV
on curve (c) is due to density of states of superconducting
tin.

lead. In particular the strong peaks at ± 6.0
and ±10.0 mV are identified with the transverse
and longitudinal phonons of the superconducting Pb
and correspond to an increase in resistance. The
fine structure or shoulders on the phonon peaks and
the broader peaks between 10 and 20 mV can be
associated with the critical points of Pb and with
the combination and harmonics of the transverse
and longitudinal phonons.[25] The symmetrical struc-
ture at ±38 mV is associated with the longitudinal
optical phonon of GaAs. The peak at reverse bias,
+ 38 mV, is in the same direction as the supercon-
ducting Pb phonons at + 6 and + 10 mV and corre-
sponds to a decrease in conductance. The peak at
forward bias – 38.2 mV corresponds to an increase
in conductance. The curves shown have not been
corrected for the energy shift due to the supercon-
ducting gap of the metal electrode. Thus in curve
(a) all structure is displaced toward higher energy

by $\Delta = 1.35$ mV, the half-width of superconducting Pb gap.

Curve (b) shows the spectra of a Sn junction taken at 4.2 °K. There is a weak resistance peak at zero bias. The structure due to GaAs phonons is at lower energy since there is no superconducting gap. Curve (c) shows the tunneling spectra of the same Sn junction at 1.2 °K. The antisymmetrical structure between 0 and ±30 mV that is not present in curve (b) is due to the density states of the superconducting tin. This structure disappears when the superconductivity of the tin is quenched by a magnetic field and one is left essentially with a curve similar to curve (b) except that the GaAs phonon structure is sharper, due to the lower temperature.

Figure 5 shows the spectra of the Pb junction in more detail and to higher voltages. The structure at the high-energy sides of the GaAs phonons shown in the inserts on expanded scale is due to the reflection of the superconducting lead density-of-states phonons at ±6 and ± 10 mV shown in Fig. 4(a). The reflected phonons at reverse bias (GaAs +) are

weaker and not as pronounced as the ones at forward bias. The metal phonon structure is reflected after every new threshold process, however, the intensity is rapidly lost. In the present case the reflected phonons are weaker approximately by a factor of 160 from the phonons at ±6 and ±10 mV. The lower curves show the structure in the presence of a magnetic field. In this case the lead density of states and the reflected phonon structure is absent and the GaAs phonons have shifted to lower energy by the half-width of the superconducting lead gap. When the lead is changed from a superconducting (upper curves) state to the normal (lower curves) state, there is a change in the background and in the line shape of the LO phonon, especially in the forward bias. The lower curve gives the line shape of the GaAs phonons for this carrier concentration, unaffected by the superconducting density of states of the lead. These line shapes, except for increased sharpness due to lower temperature, are essentially the same as shown on curve (b), Fig. 4 for a tin junction in normal state at 4.2 °K.
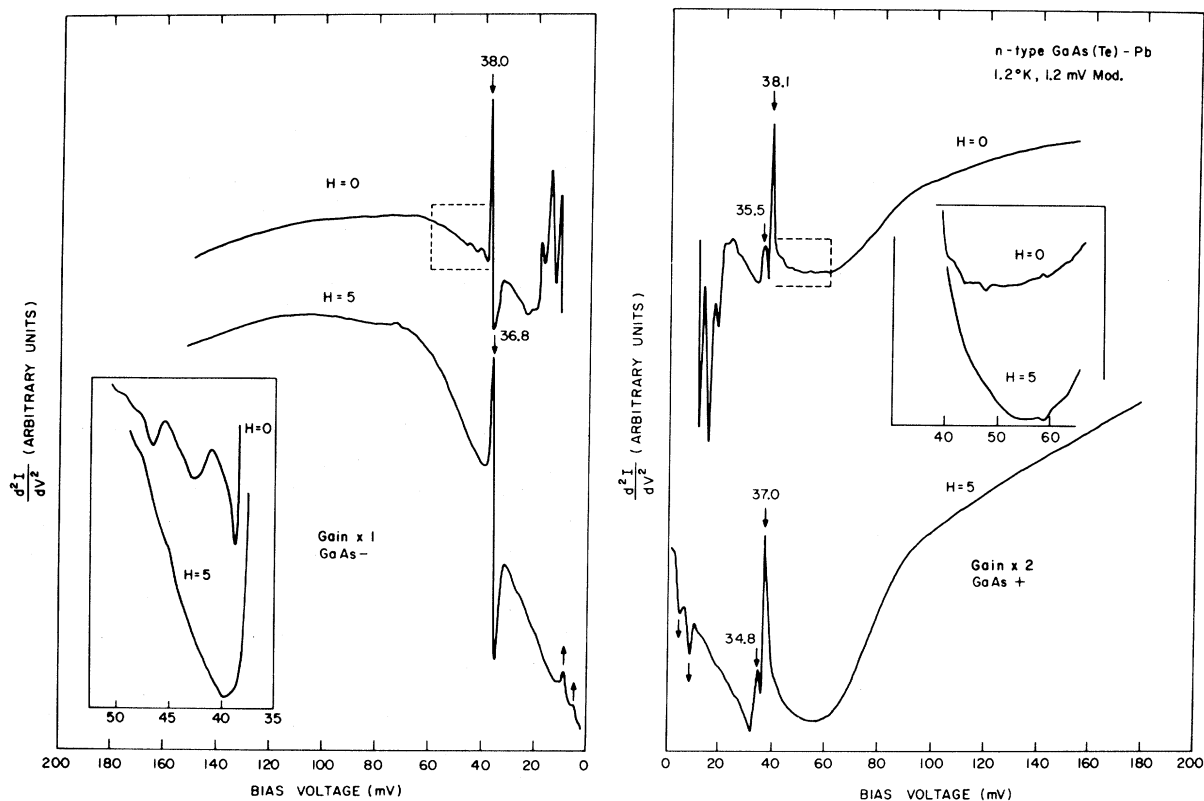

FIG. 5. Detailed spectra from Pb junction on n-type GaAs(Te) at higher voltages. The upper curves show the spectra in absence of magnetic field (Pb superconducting) and the lower curves in presence of magnetic field of 5 kOe. The structure on the high-energy side of GaAs phonons, $H = 0$, is due to reflection of the superconducting lead density-of-states phonons at ±6 and ± 10 mV. Details are shown in the inserts. The position of the broad at ± 60 mV and peak at + 90 mV is dependent on the carrier concentration of the crystal and is due to plasmons.

The position of the broad dip at +60 mV and the hump at +90 mV has been shown to be dependent on the number of carriers in the crystal. This has been interpreted variously as due to the interaction of the tunneling electron with the surface plasmons[7,26] and also with the volume plasmons.[6] We have observed this in both Se- and Te-doped samples and the results agree with the experimental data previously reported.[5,6] The broad peak and dip also occur at forward bias but are usually much weaker.

In Fig. 6 are shown the normal Pb phonons,[4] which can also be seen in Fig. 5, when the superconductivity of the lead is quenched by the magnetic field. The phonons are slightly asymmetric, occurring at -8.7, -5.4 and at $+9.1$, $+5.2$ mV. The results agree with the data from metal-oxide–Pb tunneling junctions as observed by Jaklevic and Lambe[27] and by Rowell $et\,al.$[28] The normal Pb phonons are in opposite direction to the superconducting density-of-states phonons as shown in Fig. 6, and correspond to an increase in conductance. This behavior is characteristic of inelastic tunneling processes in which the tunneling electron emits a phonon in the process of tunneling.
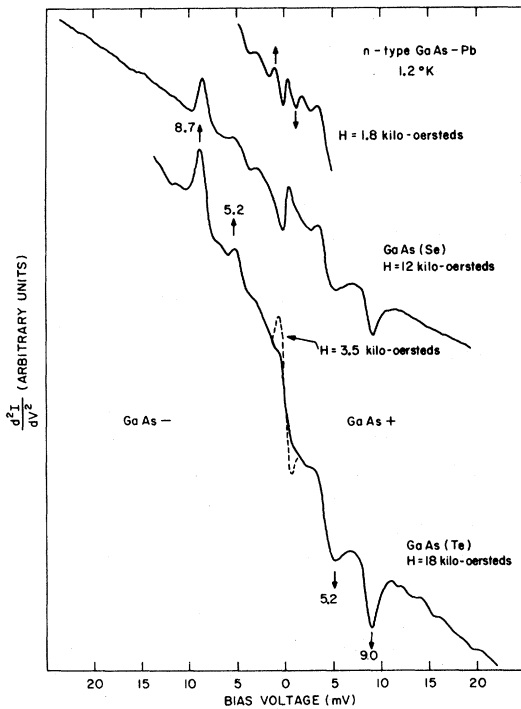
The Se-doped samples have a small conductance
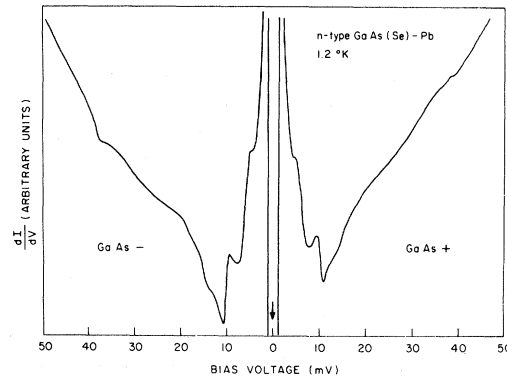
FIG. 7. Conductance or dI/dV of a typical Pb junction on n-type GaAs at 1.2 °K. The arrow at zero bias points to the large decrease in conductance due to the superconducting lead gap. The structure at ±38 mV is due to LO phonon of GaAs.

peak at zero bias, while the Te-doped samples have a small resistance peak at zero bias. The zero-bias conductance peaks are due to neutral donor impurities. If the donor is too shallow the wave function is not localized and no conduction peak is seen. This seems to be the case for Te-doped samples where the donor level lies 0.003 eV below the conduction band. If the donor level is deeper, the wave function is more localized and a conduction peak is seen.[3,29] The Se donor level lies 0.005 eV below the conduction band.

The superconductive state of lead can be quenched by a quite low magnetic field approximately of the order of 1 kOe. Very often, however, there is a residue of the superconducting Pb gap left which cannot be completely quenched except at much higher magnetic fields. This is shown on the upper curve for Se-doped sample ($H = 1.8$) and by the dotted curve for Te-doped sample ($H = 3.5$). This type of incomplete quenching of superconducting gaps has also been observed in metal-oxide–metal junctions.[28]

The first derivative dI/dV or conductance of a typical Pb junction is shown in Fig. 7. The structure near zero bias is due to the superconducting density of states of Pb, and the sharp dip at zero (off scale) is due to the Pb gap. At the position of the LO phonon of GaAs, ±38 mV, there is a sharp change in conductivity. In the forward bias (GaAs–) there is a slight decrease in conductivity followed by a sharp rise while at reverse bias there is just a step or decrease in conductance.

2. p-$Type$ GaAs

Measurements on p-type GaAs were made on zinc-doped single crystals. The nominal room-temperature carrier concentration was 4.6×10^{18}

FIG. 6. Tunneling spectra from Pb junctions on n-type GaAs showing the normal Pb phonons at -8.7, -5.2 and at $+9.0$, $+5.2$ mV. The upper curve for GaAs(Se) and the dotted curve for GaAs(Te) show incomplete quenching of the lead gap at lower magnetic fields.

per cm³. The spectra of a p-type GaAs-Al junction
at 4.2 and 1.2 °K are shown in Fig. 8. The large
peak at forward bias (GaAs +) at 37.5 mV is due to
the interaction of the tunneling electrons with the
LO phonon mode of GaAs. The small shoulder on
low-energy side of the LO phonon has been identified
by Tsui[2] as the TO mode of GaAs. The structure
at reverse bias can be seen more clearly at 1.2 °K,
as is shown in the insert.

The curves also show the typical zero bias anom-
alies seen in our junctions. At 4.2 °K there is a
small resistance peak at zero bias. As the tem-
perature is lowered a sharp conductance peak ap-
pears as shown on the bottom curve. This peak is
similar to the zero bias conductance peak observed
in n-type Se-doped GaAs and is probably due to neu-
tral acceptor centers.[3,29] Similar zero-bias anom-
alies are found in junctions made with other metals.

Figure 9 shows the spectra of the Pb junction at
forward bias at 1.2 °K. The superconducting lead
phonon structure on the high-energy side of the LO
phonon is similar to the structure seen in n-type
GaAs-Pb junctions. There is a small peak at 77
mV corresponding to twice the LO phonon energy.
With the quenching of the superconductivity of the
Pb, the GaAs phonons shift to lower energy by half-
width of Pb gap and the superconducting Pb phonon
structure and its reflection after the GaAs phonons
disappear. The GaAs structure at reverse bias is
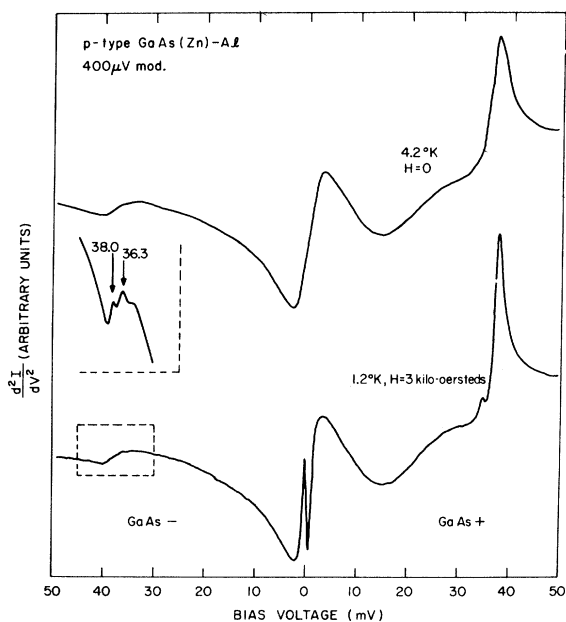the same as shown in the insert for the Al junction

FIG. 9. Tunneling spectra from Pb junction on p-type
GaAs(Zn) at forward bias at 1.2 °K. Structure at high-
energy side of GaAs phonons ($H = 0$) is due to reflection
of superconducting density-of-states structure of Pb be-
tween 6 and 20 mV. The peak at 77 mV corresponds to
twice the energy of the GaAs 1.0 phonon. The insert
shows the structure due to a resistance maximum and
incomplete quenching of the lead gap ($H = 6$ kOe) at zero
bias.

FIG. 8. Tunneling spectra from Al junction on p-type
GaAs(Zn) at 4.2 and 1.2 °K. The structure in the insert
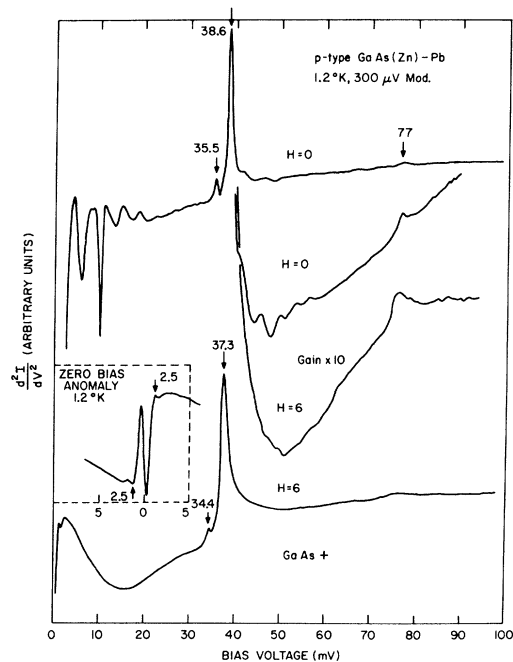shows the details of GaAs phonons at reverse bias.

in Fig. 8.

As in the case of the Al junctions, usually a small
conductance peak appears at zero bias as the tem-
perature is lowered to 1.2 °K. In addition there
is a residue left over from the quenched Pb gap at
± 2.5 mV, the peak height of which decreases slowly
with increasing magnetic field. This can be seen
in the expanded conductance curve dI/dV near zero
bias shown in Fig. 10, which shows a decrease of
the structure near zero bias with increasing mag-
netic field. The general dI/dV curves are quite
similar to the one obtained by Mahan and Conley[1]
on Au junctions.

In p-type material the GaAs LO phonon in for-
ward bias is about twice as strong as the supercon-
ducting density-of-states lead phonon at 10 mV. In
comparison with the n-type material, the GaAs
phonon at forward bias (GaAs −) is weaker than the
superconductive Pb phonon approximately by a fac-
tor of 3 and in reverse bias (GaAs +) weaker by a
factor of 7 or 8. No second harmonic peak of the
LO phonon is seen in n-type material. This is in
contrast with the p-type material where the peak at
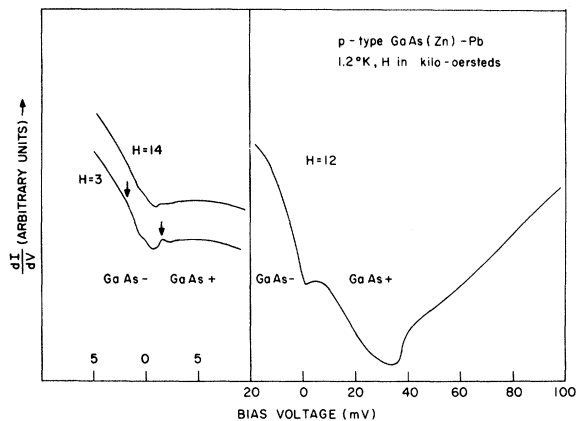twice the LO phonon energy is down approximately

FIG. 10. Conductance or dI/dV of a Pb junction in the normal state on p-type GaAs at 1. 2 °K. The curves on the left show the effect of magnetic field in reducing the structure left over from the quenched Pb gap.

by a factor of 80 in intensity from the LO phonon. The zero-bias anomalies are also stronger in p-type material than in n-type. It is also interesting to note that no normal Pb phonons are seen on p-type material while they are quite easily seen on n-type material. The normal Pb phonons may be masked by the large zero-bias anomaly that is present in the p-type materials.

3. n-Type GaSb

Figure 11 shows the spectra of an Au junction at 4. 2 °K and an Sn junction in the presence of a magnetic field at 1. 2 °K made on n-type GaSb(Te), with a nominal carrier concentration of 1×10^{18} per cm^2. The salient feature of this spectra is the LO phonon at 30 mV which occurs at both forward and reverse bias. The peak at reverse bias (GaSb +) corresponds to an increase in resistance and the one in
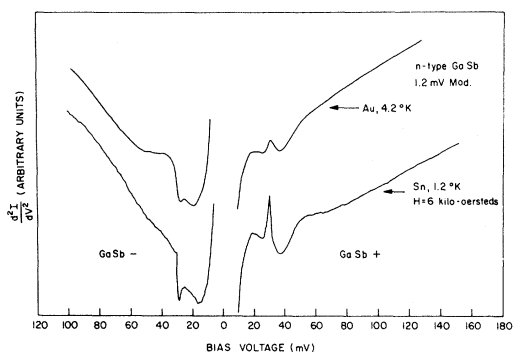

FIG. 11. Tunneling spectra from Au junction at 4. 2 °K and Sn junction, in presence of magnetic field, at 1. 2 °K, on n-type GaSb(Te).
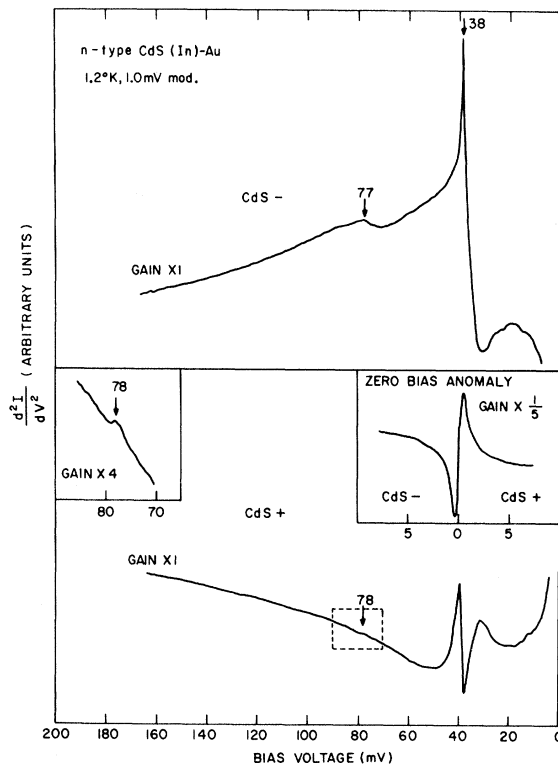

FIG. 12. Tunneling spectra from Au junction on n-type CdS(In) at 1. 2 °K. Structure occurs at the LO phonon energy (± 38 mV) and at twice the LO phonon energy in both forward and reverse bias.

forward bias to an increase in conductance. The dip at + 38 mV and the rise to broad peak at 52 mV is similar to the plasma mode seen in GaAs. A simple calculation using $\omega_p = (4\pi n/m^*\epsilon_\infty)^{1/2}e$, where[30] m^* = 0. 047, and $\epsilon_\infty = 1.$ 64 gives a value of $\omega_p = 42$ mV for $n = 9.8 \times 10^{17}$ per cm^3. The infrared reflectivity has a minimum at 40 mV for the same sample. This calculation would put the volume plasmon at observed conduction maxima and surface plasmon in the region of the LO phonon.

4. n-Type CdS

Measurements were made on indium-doped CdS both on air-cleaved and on chemically etched polished surfaces. Figure 12 shows the spectra of an Au junction on a polished and etched surface at 1. 2 °K both at forward and reverse bias. Prominent structure occurs at the LO phonon energy of CdS. The line shapes are similar to those observed by Losee and Wolf[3] on junctions prepared on vacuum-cleaved faces. A broad peak at twice the LO phonon energy is observed at both forward and reverse bias. The zero-bias conductance peak due to neutral donors[3] in the barrier is shown in the insert.
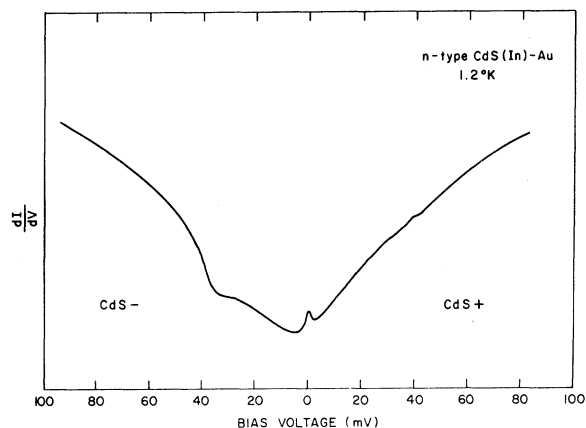
FIG. 13. Conductance or dI/dV of an Au junction on n-type CdS. The structure near ± 38 mV is due to the LO phonons of CdS.

Typical conductance curve dI/dV for an Au junction on CdS is shown in Fig. 13.

5. n-Type SnO$_2$

Figures 14 and 15 show the d^2I/dV^2 spectra of a lead tunnel junction made on an antimony-doped degen-
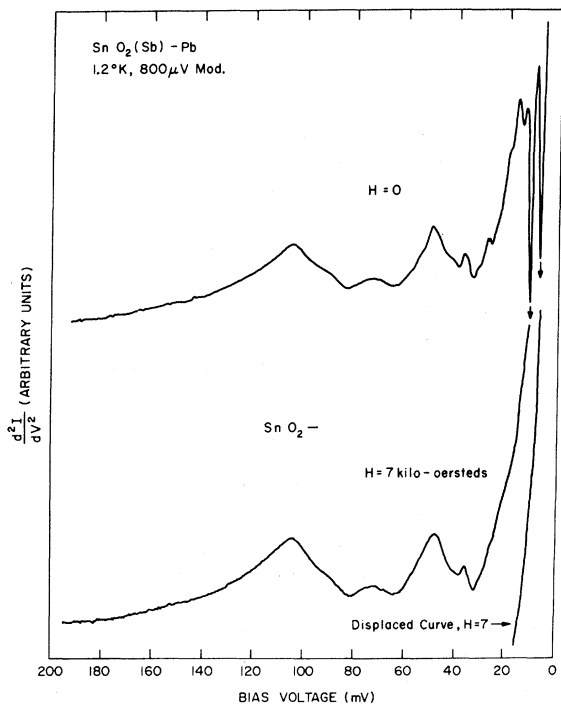

FIG. 15. Tunneling spectra of the SnO$_2$-Pb junction at 1.2 °K in reverse bias.

erate single crystal of SnO$_2$.[31] The junctions were made on faces parallel to the c axis of the crystal. The two sharp peaks at ± 6 and ± 10 mV on the upper curves are due to the transverse and longitudinal superconducting lead density-of-states phonons. The superconducting lead density-of-states structures extends to about ± 22 mV. All of this structure disappears when the lead is quenched from the superconducting to the normal state by a magnetic field. This is shown on the lower curves and the structure that is left is due to SnO$_2$.

Tin oxide has a rutile crystal structure. The unit cell consists of six atoms, four oxygen and two titaniums. There are three basic motions of the ions in the unit cell in the direction perpendicular to the c axis and a single type of motion parallel to the c axis.[32] The transverse and longitudinal modes associated with these basic motions have been identified from the infrared reflectivity data by van Daal.[33] The infrared results and the positions of conductance peaks shown in Figs. 14 and 15 are summarized in Table II.

The structure is much weaker in the reverse bias (SnO$_2$ +) than in the forward bias. The agreement between the lattice vibrational frequencies obtained from infrared reflectivity data and conductance peaks in d^2I/dV^2 spectra is fair. The identification of the conductance peaks with the lattice vibrations has to remain tentative since the peaks are rather

FIG. 14. Tunneling spectra of an n-type SnO$_2$(Sb)-Pb junction at 1.2 °K at forward bias. In the lower curve the superconducting lead density-of-states phonons at 6 and 10 mV has been quenched by the magnetic field.
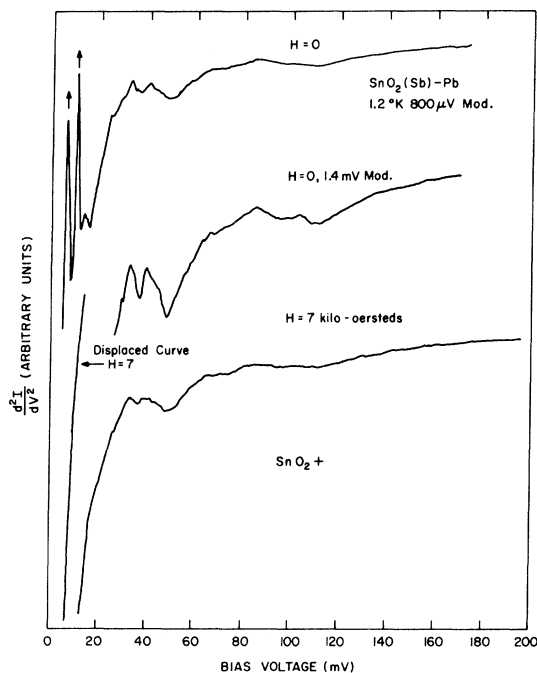
TABLE II. Values of lattice vibrations of SnO_2 from infrared data by Van Daal (Ref. 33) and positions of conductance peaks in d^2I/dV^2 curves shown in Figs. 14 and 15.

Mode	Frequency (mV) (infrared)	Conductance peaks in d^2I/dV^2	
		SnO_2-	Sn_2O+
$T_\perp^{(1)}$	28.5	28 ?	
$L_\perp^{(1)}$	34.2		
$T_\perp^{(2)}$	34.8	35	36
$L_\perp^{(2)}$	45.2	48	48
$T_\parallel$	55.8	···	···
$T_\perp^{(3)}$	72.5	76	70 sh
$L_\parallel$	86.2	···	···
$L_\perp^{(3)}$	93.0	93 sh	93
···	···	104	~108

broad and it is not clear whether the interaction between the tunneling electron and the lattice would produce conductance dips or peaks.

B. Junctions Doped with Molecular Impurities

Recently, Thompson[34] has claimed to have observed rotational modes of HCl in GaAs point tunnel contacts. One of the advantages of the metal-semiconductor junction is that the tunneling barrier is formed within the semiconductor itself. The junctions are mechanically more rugged and stable than the metal-oxide—metal junctions, mainly because the thin oxide barriers are quite fragile and are easily damaged. The Schottky barriers have also an advantage in that one does not have the problem of barrier breakdown with applied voltage. This is a major problem in oxide barriers where breakdown can occur at thin spots in the oxide. Thus the metal-semiconductor junction would have a definite advantage as a spectroscopic tool over the metal-oxide—metal junctions if one could use it to observe vibrational modes of impurities introduced into the junctions. We have doped junctions made on n- and p-type GaAs and on n-type CdS with molecular impurities, in hope of observing the vibrational modes of the impurity molecules. The junctions are made on polished and etched surfaces of the crystal which are then heated in vacuum in order to drive off adsorbed gases on the surface, and then cooled down to room temperature before exposure to or evaporation of the impurity molecules and the metal electrodes. The whole evaporation process is monitored with a crystal quartz microbalance, which gives the relative amount of material evaporated. The impedances of the doped junctions were at least one order of magnitude higher than that of the clean junctions.

We have used impurities that have worked well in metal-oxide—metal junctions.[8] Most of the work was done on copper-phthalocyanine, but we have also studied junctions doped with pump oil and acetic and propionic acids in hope of observing C-H rock, bending, and stretching modes, so far with negative results. The phthalocyanine molecule is a large, flat, square, and nearly planar molecule. The nucleus consists of a central conjugated azaporphyrin ring which is regarded as the chromophore, surrounded by four fuzed benzene rings. The central azaporphyrin ring is filled with a metal atom, or complex for metallic derivatives or with two hydrogen atoms for the case of metal-free phthalocyanine. Figure 16 shows the structure for copper-phthalocyanine $(C_8H_4N_2)_4Cu$.

The phthalocyanines have high thermal and chemical stability and are insoluble in common solvents. They sublime unchanged at ~ 400 °C and 10^{-6}-mm pressure. Copper-phthalocyanine is stable up to 900 °C in vacuum. Phthalocyanines have strong absorption in the region of 6650 to 7150 Å giving them a greenish-blue color and are commonly used as dyes which are known for their resistance to fading.

The infrared spectra of phthalocyanine is quite complicated. Besides C-H, N-H modes and C-C benzene ring skeletal vibrations,[35] there are three fairly strong peaks at 54.5, 63, and 71 mV at room temperature. These also show up in d^2I/dV^2 spectra of metal-oxide—metal junction doped with phthalocyanine shown in Fig. 17.[36]

Figure 18 shows the spectra of a Pb junction on p-type GaAs and Fig. 19 shows spectra of a Pb junction on n-type CdS both doped with Cu-phthalocyanine. Both junctions show the LO phonons of the semiconductor and the superconducting Pb gap
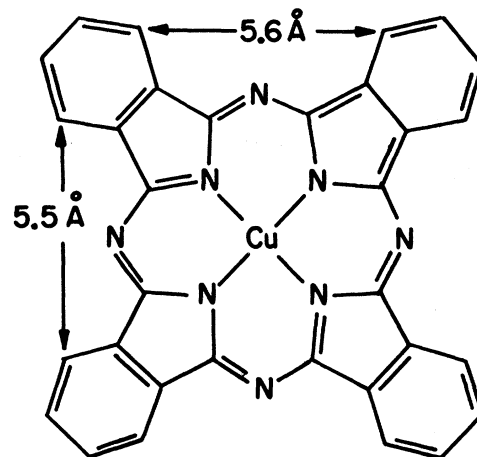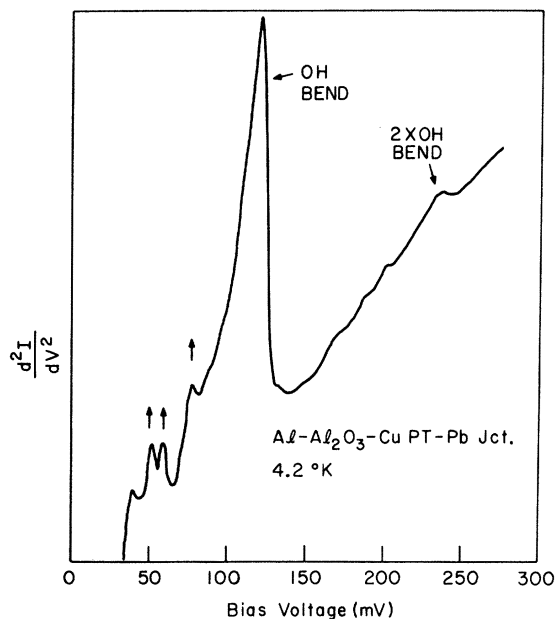

FIG. 16. Structure of copper-phthalocyanine $(C_8H_4N_2)_4$ Cu.

FIG. 17. Tunneling spectra of Al-Al$_2$O$_3$-Pb junction doped with phthalocyanine after Jaklevic and Lambe (Ref. 36).

FIG. 18. Tunneling spectra from Pb junction on p-type GaAs doped with copper phthalocyanine at 1.2 °K.

indicating that the doped junction is still a tunnel junction. However we were not able to identify any peaks as due to phthalocyanine in the range from 50 to 80 mV. This is true both in GaAs where the bar-
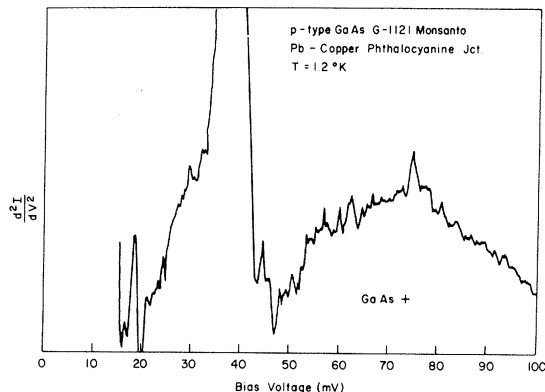
rier height is surface state dominated and in CdS where the surface states and barrier height depends more on the work function of the metal. Exposing the samples to air after heating but before evaporation of phthalocyanine made no difference in the results. Admittedly not all the parameters specifying the junctions are known or controlled. The extent of the role played by surface states, dislocations, contamination, and surface chemistry between the impurities and the surfaces of the crystals in suppressing the observation of molecular vibrations is unknown and should be studied further.
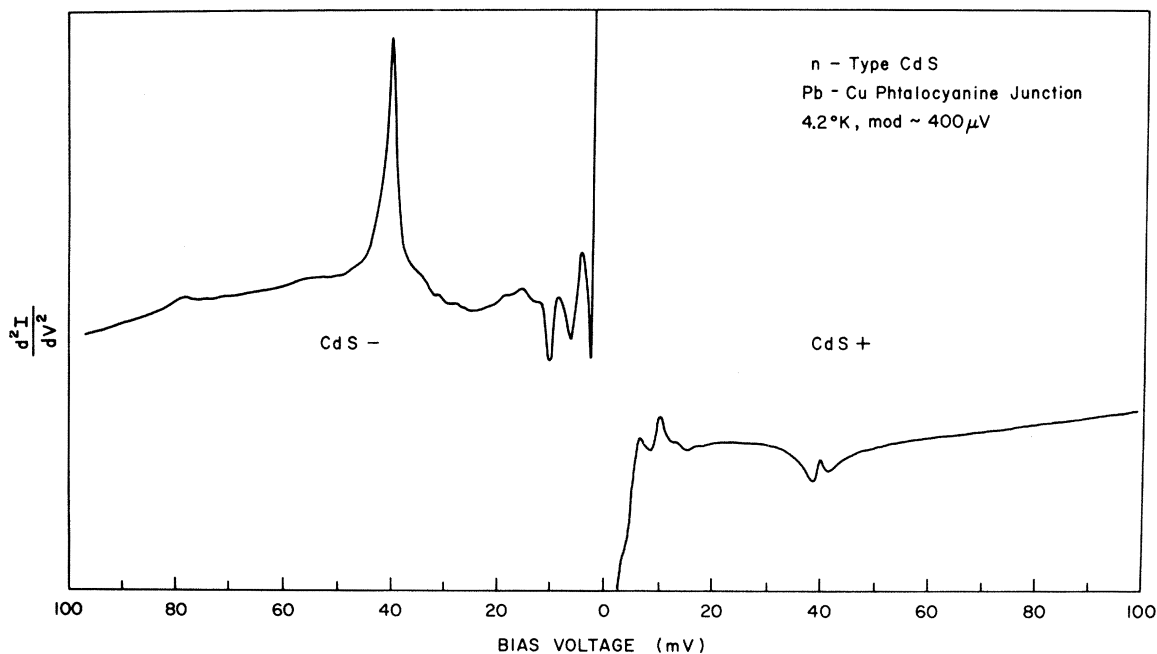

FIG. 19. Tunneling spectra from Pb junction on n-type CdS doped with copper phthalocyanine at 4.2 °K.

SUMMARY

The technique of forming a Schottky barrier tunnel junction by evaporating metal contacts on the crystal whose surfaces have been cleaned by heating in vacuum has been successfully used on GaAs, GaSb, and CdS. On the other hand no elaborate cleaning treatment is necessary to form good tunnel junctions on SnO_2. All of these junctions show the detailed superconducting structure of the metal electrodes and the phonon structure associated with the optical modes of the semiconductor.

Attempts to observe the vibrational structure of molecular impurities introduced into the junctions proved to be unsuccessful. This is in contrast to results obtained from metal-oxide–metal junctions. At present we are unable to account precisely for these results. Further study of the surface chemistry and properties of the metal semiconductor interface seems necessary.

[1]J. W. Conley and G. D. Mahan, Phys. Rev. 161, 681 (1967).

[2]D. C. Tsui, Phys. Rev. Letters 21, 994 (1968).

[3]D. L. Losee and E. L. Wolf, Phys. Rev. 187, 925 (1969).

[4]M. Mikkor and W. C. Vassell, Bull. Am. Phys. Soc. 14, 43 (1969).

[5]L. C. Davis and C. B. Duke, Phys. Rev. 184, 764 (1969).

[6]C. B. Duke, M. J. Rice, and F. Steinrisser, Phys. Rev. 181, 733 (1969).

[7]D. C. Tsui, Phys. Rev. Letters 22, 293 (1969).

[8]J. Lambe and R. C. Jaklevic, Phys. Rev. 165, 821 (1968).

[9]C. E. Jones and A. R. Hilton, J. Electrochem. Soc. 112, 908 (1965).

[10]H. C. Gatos, M. C. Lavine, and E. P. Warekois, J. Electrochem. Soc. 108, 645 (1961).

[11]D. F. Kyser and M. F. Millea, J. Electrochem. Soc. 111, 1102 (1964).

[12]A. U. MacRae and G. W. Gobeli, J. Appl. Phys. 35, 1629 (1964).

[13]F. Jona, IBM J. Res. Develop. 9, 375 (1965).

[14]A. U. MacRae, Surface Sci. 4, 247 (1966).

[15]C. D. Thurmond, J. Phys. Chem. Solids 26, 785 (1965).

[16]E. P. Warekois, M. C. Levine, A. N. Maiano, and H. C. Gatos, J. Appl. Phys. 37, 2203 (1966); 33, 690 (1962).

[17]B. D. Campbell and H. E. Farnsworth, Surface Sci. 10, 197 (1968).

[18]J. Shappir and A. Many, Surface Sci. 14, 169 (1969).

[19]R. Schubert, Phys. Status Solidi 16, K157 (1966).

[20]W. G. Spitzer and C. A. Mead, J. Appl. Phys. 34, 3061 (1963); D. V. Geppert, A. M. Cowley, and B. V. Dore, ibid. 37, 2458 (1966).

[21]A. Many and A. Katzir, Surface Sci. 6, 279 (1967).

[22]J. A. Marley and R. C. Dockerty, Phys. Rev. 140, A304 (1965).

[23]W. R. Patterson and J. Sheuchun, Rev. Sci. Instr. 35, 1704 (1964); D. E. Thomas and J. M. Rowell, ibid. 36, 1301 (1965); J. G. Adler and J. E. Jackson, ibid. 37, 1049 (1966).

[24]A. M. Goodman, J. Appl. Phys. 36, 1411 (1965).

[25]J. M. Rowell and L. Kopf, Phys. Rev. 137, A907 (1965).

[26]K. L. Ngai, E. N. Economou, and M. H. Cohen, Phys. Rev. Letters 22, 1375 (1969).

[27]R. C. Jaklevic and J. Lambe (private communication); Bull. Am. Phys. Soc. 14, 43 (1969).

[28]J. M. Rowell, W. L. McMillan, and W. L. Feldman, Phys. Rev. 180, 658 (1969).

[29]E. L. Wolf and D. L. Losee, Solid State Commun. 7, 665 (1969).

[39]Values from American Institute of Physics Handbook (McGraw-Hill, New York, 1963), 2nd ed.

[31]The single crystals were kindly supplied by Dr. J. A. Marley, Corning Glass Works, Corning, N. Y.

[32]D. M. Eagles, J. Phys. Chem. Solids 25, 1243 (1964).

[33]H. J. van Daal, Solid State Commun. 6, 5 (1968).

[34]W. A. Thompson, Phys. Rev. Letters 20, 1085 (1968).

[35]A. B. P. Lever, Advan. Inorg. Chem. Radiochem. 1, 27 (1965).

[36]R. C. Jaklevic and J. Lambe (unpublished).